Hydrol. Earth Syst. Sci. Discuss., 12, 7933–7969, 2015
www.hydrol-earth-syst-sci-discuss.net/12/7933/2015/
doi:10.5194/hessd-12-7933-2015
© Author(s) 2015. CC Attribution 3.0 License.

Hydrology and Earth System Sciences
Open Access
Discussions

This discussion paper is/has been under review for the journal Hydrology and Earth System Sciences (HESS). Please refer to the corresponding final paper in HESS if available.

Influence of climate variability on water partitioning and effective energy and mass transfer (EEMT) in a semi-arid critical zone

X. Zapata-Rios[1], P. D. Brooks[2,1], P. A. Troch[1], J. McIntosh[1], and C. Rasmussen[3]

[1]Department of Hydrology and Water Resources, The University of Arizona, Tucson, Arizona, USA
[2]Department of Geology and Geophysics, University of Utah, Salt Lake City, Utah, USA
[3]Soil, Water and Environmental Science, The University of Arizona, Tucson, Arizona, USA

Received: 25 June 2015 – Accepted: 15 July 2015 – Published: 17 August 2015

Correspondence to: X. Zapata-Rios (xavierzapata@email.arizona.edu)

Published by Copernicus Publications on behalf of the European Geosciences Union.

CC BY

Abstract

The Critical Zone (CZ) is the heterogeneous, near-surface layer of the planet that regulates life-sustaining resources. Previous research has demonstrated that a quantification of the influxes of effective energy and mass (EEMT) to the CZ can predict its structure and function. In this study, we quantify how climate variability in the last three decades (1984–2012) has affected water availability and the temporal trends in EEMT. This study takes place in the 1200 km^2 upper Jemez River Basin in northern New Mexico. The analysis of climate, water availability, and EEMT was based on records from two high elevation SNOTEL stations, PRISM data, catchment scale discharge, and satellite derived net primary productivity (MODIS). Records from the two SNOTEL stations showed clear increasing trends in winter and annual temperatures (+1.0–1.3 °C $decade^{-1}$; +1.2–1.4 °C $decade^{-1}$, respectively), decreasing trends in winter and annual precipitation (–41.6–51.4 mm $decade^{-1}$; –69.8–73.2 mm $decade^{-1}$, respectively) and maximum Snow Water Equivalent (SWE; –33.1–34.7 mm $decade^{-1}$). The water partitioning fluxes at the basin scale showed statistically significant decreasing trends in precipitation (–61.7 mm $decade^{-1}$), discharge (–17.6 mm $decade^{-1}$) and vaporization (–45.7 mm $decade^{-1}$). Similarly Q_{50}, an indicator of snowmelt timing, is occurring 4.3 days $decade^{-1}$ earlier. Results from this study indicated a decreasing trend in water availability, a reduction in forest productivity (4 g C m^{-2} per 10 mm of reduction in Precipitation) and EEMT (1.2–1.3 MJ m^2 $decade^{-1}$). These changes in EEMT point towards a hotter, drier and less productive ecosystem which may alter critical zone processes in high elevation semi-arid systems.

1 Introduction

The critical zone (CZ) is the surficial layer of the planet that extends from the top of the vegetation canopy to the base of aquifers (Chorover et al., 2011; Brandley et al., 2007). Within its boundaries complex interactions between air, water, biota, organic

CC BY

matter, soils and rocks take place that are critical for sustaining live on Earth (Brandley et al., 2007). The CZ has been conceptualized and studied as a weathering engine or reactor where interacting chemical, physical and biological processes drive weathering reactions (Anderson et al., 2007; Chorover et al., 2011). Over long time scales, the CZ has evolved in response to climatic and tectonic forces and has been recently influenced by human activities (Steffen et al., 2007). Understanding how climate and land use changes affect CZ structure and related processes has become a priority for the science community due to the implications it may have on the functioning of life supporting resources. It has been hypothesized by the researchers from the Jemez River Basin (JRB) – Santa Catalina Mountains (SCM) Critical Zone Observatory (CZO) (http://criticalzone.org/catalina-jemez/) that a quantification of the inputs of the effective energy and mass transfer (EEMT) to the CZ can provide insight about its structure and function (Chorover et al., 2011). CZ areas that receive greater EEMT influxes have been shown to have greater structural organization as well as more dissipative products leaving it (Rasmussen et al., 2011; Zapata-Rios et al., 2015a). The opposite has been observed in regions with less EEMT.

EEMT is a variable that quantifies energy and mass transfer to the critical zone (Rasmussen et al., 2011). EEMT integrates within a single variable the energy and mass associated with water in excess from evapotranspiration, quantified as effective precipitation (E_{ppt}), and reduced carbon compounds resulting from primary production (E_{bio}) (Rasmussen et al., 2011). It has been demonstrated that other possible energy fluxes to the CZ such as potential energy from transport of sediments, geochemical potential of chemical weathering, external inputs of dust, heat exchange between soil and atmosphere, and other sources of energy coming from anthropogenic sources are orders of magnitude smaller (Phillips, 2009; Rasmussen et al., 2011; Rasmussen, 2012). Therefore the two dominant terms embodied in EEMT are E_{ppt} and E_{bio}.

Previous research has shown that EEMT can become a tool to predict regolith depth, rate of soil production and soil properties (Rasmussen et al., 2005, 2011; Pelletier and Rasmussen, 2009a, b; Rasmussen and Tabor, 2007). For instance, strong correlations

HESSD
12, 7933–7969, 2015

cc BY

were found between EEMT, soil carbon, and clay content in soils on igneous parent materials from California and Oregon (Rasmussen et al., 2005). Furthermore, transfer functions were successfully determined between EEMT and pedogenic indices, including pedon depth, clay content, and chemical indices of soil alteration along an environmental gradient on residual igneous parent material (Rasmussen and Tabor, 2007). EEMT has also been incorporated in geomorphic and pedogenic models on granitic rocks to describe landscape attributes and regolith thickness (Pelletier and Rasmussen, 2009a, b). Rasmussen and Tabor (2007) demonstrated that regolith depth on stable low gradient slopes increased exponentially with increasing EEMT. Similarly, Pelletier et al. (2013) found that high EEMT values are associated with large above ground biomass, deeper soils, and longer distance to the valley bottoms across hillslopes in the Santa Catalina Mountains in southern Arizona. More recently, EEMT estimations haven been strongly correlated with water transit times, water solutes concentrations and dissolution of silicates on a rhyolitic terrain in northern New Mexico (Zapata et al., 2015a). In these studies, the main constituents of EEMT (E_{ppt} and E_{bio}) were quantified as an average value based on climate records from long-term regional databases as these variables exert first-order controls on photosynthesis and effective precipitation (Rasmussen et al., 2011; Chorover et al., 2011).

It is still uncertain how climate variability influences CZ structure and function (Chorover et al., 2011). Climate variability might directly influence changes in the transfer of mass and energy to the CZ as climate has a direct control on both E_{ppt} and E_{bio}. In the mountains of the southwestern United States, a large percentage of annual precipitation falls as snow, which is stored during the winter and released as snowmelt during the spring (Clow, 2010). The water from the winter snowpack constitutes the main source of regional water supplies and the largest component of runoff (Bales et al., 2006; Nayak et al., 2010). The regional snowpack has been documented to be declining in the southwestern US (Mote et al., 2005; Clow, 2010) and alterations to the snowpack are likely to produce changes in vegetation, impact water availability (Bales et al., 2006; Harpold et al., 2012; Trujillo et al., 2012) and influence inputs of EEMT. For

HESSD
12, 7933–7969, 2015

cc BY

instance, significant increasing trends in air temperature and decreasing trends in winter precipitation in the last decades have been documented in the Upper Rio Grande region in northern New Mexico (Harpold et al., 2012).

The objective of this study was to evaluate climate variability and its influence on the temporal changes of water partitioning and EEMT at the catchment scale in a semi–arid CZ over the last few decades. This investigation took place in the upper part of the Jemez River Basin in northern New Mexico, a basin dominated by a forest cover and limited human infrastructure. Micro-climate variability was studied based on daily records from two SNOTEL stations using records from 1984 through 2012. Water availability and EEMT were estimated during the same time period based on precipitation and temperature from the precipitation-elevation regressions on independent slopes model (PRISM), empirical daily observations of catchment scale discharge, and satellite derived net primary productivity (MODIS).

2 Methods

2.1 Study site

The Jemez River is a tributary of the upper reach of the Rio Grande and is located between Jemez and Sierra Nacimiento Mountains in northern New Mexico (Fig. 1a). Its headwaters originate within the 360 km^2 Valles Caldera National Preserve which contains 30 % of the total basin surface (Fig. 1b). The upper Jemez River Basin is located at the southern margin of the Rocky Mountains ecoregion between latitudes 35.6 and 36.1° N and longitudes −106.3 and −106.9° W. The basin is characterized by a mean elevation of 2591 m and a gradient in elevation ranging from 1712 to 3435 m. Based on a 10 m digital elevation model, the catchment drains 1218 km^2 above the US Geological Survey (USGS) gauge "Jemez River near Jemez" (35.66° N and 106.74° W; USGS 08324000) located at an elevation of 1712 m. The basin has a predominant south aspect and a mean catchment slope of 13.7°. The geology consists of rocks

CC BY

of volcanic origin with predominant andesitic and rhyolitic compositions that overlie tertiary to Paleozoic sediments along the western margin of the Rio Grande rift (Shevenell et al., 1987). Common soil types in the basin include Aridisols, Alfisols, Mollisols and Inceptisols (Allen et al., 1991, 2002). Precipitation has a bimodal pattern with 50 % of annual precipitation occurring during the winter months (primarily as snow) from October to April and originates from westerly frontal systems. The remaining 50 % of precipitation falls as convectional rainfall during the monsoon season between July and September (Sheppard, 2002). According to the National Land Cover Database (NLCD), the basin is a forested catchment with 79 % under evergreen, deciduous and mixed forest cover and only 0.5 % of area covered by development and agriculture (http://www.mrlc.gov/nlcd06_leg.php) (Table 1).

2.2 Climatological stations

There are two Natural Resources Conservation Service snowpack telemetry (SNOTEL) stations within the study area with long-term records since 1980 (http://www.wcc.nrcs.usda.gov/snow/; Fig. 1b). The Quemazon station is located at an elevation of 2896 m (35.92° N and 106.39° W) and the Señorita Divide#2 station is located at an elevation of 2622 m (36.00° N and 106.83° W). The stations collect real-time precipitation, snow water equivalent (SWE), air temperature, soil moisture and temperature, and wind speed and direction. Air temperature records began at the Señorita Divide#2 in 1988 and at the Quemazon station in 1989. There are no stations with long-term records at the lower part of the basin.

2.3 Climate variability

Climate variability was studied based on 13 variables from the two SNOTEL stations, derived from daily air temperature, precipitation, and maximum SWE, following a similar methodology and data processing procedure as in Harpold et al. (2012). The variables analyzed were winter, summer and annual air temperature (°C), annual and winter

CC BY

precipitation (mm), maximum SWE (mm), maximum SWE to winter precipitation ratio (–), 1 April SWE (mm), first day snow cover (water year day), last day snow cover (water year day), length of snow on the ground (number of days) and SM50, which is the day of the year in which half of the snowpack melts (number of days). Climate records for data analysis were aggregated by water year (from 1 October to 30 September). Winter season was considered to be between October and April and summer season between May and September. The analysis of climate was conducted from 1984 as a starting year to avoid the anomalous wet years recorded at the beginning of 1980s that were caused by the Pacific Decadal Oscillation (PDO) and El Niño–Southern Oscillation (ENSO) (Harpold et al., 2012; and references therein). The presence of a monotonic increasing or decreasing trend in the 13 climate variables recorded at the two individual stations was evaluated from 1984 through 2012 by applying the nonparametric Mann–Kendall test with a $\alpha = 0.10$ level of significance and the nonparametric Sen's slope estimator of a linear trend (Yue et al., 2012; Sen, 1968).

2.4 EEMT estimation

In this investigation EEMT was calculated as the sum of E_{ppt} and E_{bio} (Eq. 1). We applied two different methods to estimate E_{ppt} and E_{bio}. Following a similar methodology described in Rasmussen and Gallo (2013), EEMT_{emp} was empirically estimated at the catchment scale based on baseflow estimations and average basin scale net primary productivity (NPP) derived from MODIS satellite data. In comparison, $\text{EEMT}_{\text{model}}$ was estimated at the catchment scale based on long term climate records from **P**recipitation elevation **R**egressions on **I**ndependent **S**lopes **M**odel (PRISM) developed by the climate group at Oregon State University (http://prism.oregonstate.edu/) and described in Rasmussen et al. (2005, 2011).

$$\text{EEMT} = E_{\text{ppt}} + E_{\text{bio}} \left(\text{J}\,\text{m}^{-2}\text{s}^{-1}\right) \tag{1}$$

CC BY

2.4.1 EEMT_{emp}

Upper Jemez River Basin precipitation and air temperature from 1984 through 2012 was obtained using PRISM data at an 800 m spatial resolution (Daly et al., 2002). Daily discharge data was available from 1984 through 2012 from the USGS Jemez River near Jemez gauge station (http://waterdata.usgs.gov/nwis). The upper Jemez River has not been subjected to flow regulation and almost 60 % of the annual discharge occurs during the snowmelt period between March and May. Daily discharge records were normalized by catchment area and mean daily discharge was aggregated into water years.

Catchment scale water partitioning fluxes (1984–2012) were calculated following the Horton index approach of Troch et al. (2009) and Brooks et al. (2011). The Horton index is an indicator of water partitioning at the catchment scale and integrates both effects of landscape and vegetation in water partitioning (Voepel et al., 2011). The Horton index represents a metric of catchment scale vegetation water use and was calculated as follows:

$$\text{HI} = \frac{V}{W} = \frac{P - Q}{P - S} \tag{2}$$

where, V represents vaporization, W catchment wetting, P catchment scale precipitation, Q discharge and S quickflow.

Precipitation (P) on the land surface was partitioned between quickflow (S) and catchment wetting (W). S represents water that directly contributes to streamflow discharge as a response to precipitation events, thus this amount of water is not transferred to the critical zone. W is the total amount of water that infiltrates the soil, of which a portion is available for vaporization (V) including vegetation uptake. The remaining portion of W flows though the critical zone and contributes to baseflow (U). V was estimated at the annual scale as the difference between P and discharge (Q). Q was separated between S and U using a one-parameter low-pass filter (Lyne and

HESSD
12, 7933–7969, 2015

cc BY

Hollick, 1979; Arnold and Allen, 1999; Eckhardt, 2005; Troch et al., 2009) (Eq. 3).

$$U_k = aU_{k-1} + \frac{1-a}{2}\left(Q_k - Q_{k-1}\right) \tag{3}$$

$$U_k \leq Q_k$$

where a is a filter parameter set to 0.925. This filter was passed twice, backward and forward in time to improve the partitioning of U and S at the beginning of the time series. After this, daily values of Q, U, and S were integrated to annual time scales. Alterations in snowmelt timing were evaluated with Q_{50}, which indicates the day of the water year when 50 % of the total annual discharge is recorded at the catchment outlet (Clow, 2010; Stewart et al., 2004).

The term $E_{\text{ppt\_emp}}$ was calculated as stated in Eq. (4) based on estimations of U and mean PRISM derived air temperature at the catchment scale (Rasmussen et al., 2011; Rasmussen and Gallo, 2013).

$$E_{\text{ppt}} = U \cdot C_{\text{w}} \cdot \Delta T \, (\text{J}\,\text{m}^{-2}\,\text{s}^{-1}) \tag{4}$$

In Eq. (4), C_{w} is the specific heat of water (4187 $\text{J}\,\text{kg}^{-1}\,\text{K}^{-1}$) and ΔT is the difference in temperature between ambient temperature and 0 °C calculated as $T_{\text{ambient}} - T_{\text{ref}}$ (273.15 °K).

Net primary productivity

Mean annual NPP at the catchment scale was estimated at a 1 km spatial resolution for the years 2000 through 2012 using data MOD17A3 from MODIS (Zhao and Running, 2010) (http://modis-land.gsfc.nasa.gov/npp.html). E_{bio} was calculated as indicated in Eq. (5) and presented in Rasmussen et al. (2011) and Rasmussen and Gallo (2013).

$$E_{\text{bio}} = \text{NPP} \cdot h_{\text{bio}} \left(\text{J}\,\text{m}^{-2}\,\text{s}^{-1}\right) \tag{5}$$

HESSD
12, 7933–7969, 2015

where, h_{bio} is the specific biomass enthalpy and equivalent to $22\,\mathrm{kJ\,m^{-2}\,s^{-1}}$ (Lieth, 1975; Phillips, 2009). As MODIS data was only available from the year 2000 onwards, single and multivariate linear regression analysis were estimated with the objective of finding a statistical model to extend E_{bio_emp} records back to 1984. Using a similar approach as Rasmussen and Tabor (2007), linear regressions were explored between E_{bio_emp} and climate variables from the SNOTEL stations and the entire basin.

2.4.2 EEMT$_{\mathbf{model}}$

E_{ppt_model} was calculated based on estimations of effective precipitation (P_{eff}) which is defined as the amount of water that enters the CZ in excess of evapotranspiration and is available to flow through the CZ (Rasmussen et al., 2005; Eq. 6)

$$E_{ppt\_model(i)} = P_{eff(i)} \cdot C_w \cdot \Delta T \tag{6}$$

where $P_{eff(i)}$ is monthly effective precipitation calculated as the difference between monthly PRISM precipitation and monthly potential evapotranspiration calculated using the Thornthwaite equation (Rasmussen et al., 2005; Thornthwaite, 1948). C_w and ΔT are the same parameters described in Eq. (4). $E_{ppt\_model(i)}$ was calculated on a monthly basis only for the months when precipitation is larger than evapotranspiration ($P_{eff(i)} > 0$) and these values were integrated in water years. E_{bio_model} was estimated as indicated in Eq. (5) and NPP was calculated following an empirical relationship based on air temperature (Eq. 7; Lieth, 1975).

$$\mathrm{NPP}(i) = \frac{3000}{1 + e^{1.315 - 0.119 T_a}} \cdot \frac{\mathrm{days}(i)}{365 \frac{\mathrm{days}}{\mathrm{year}}} \tag{7}$$

NPP(i) is monthly NPP in $\mathrm{g\,m^{-2}\,yr^{-1}}$ and T_a is monthly air temperature. $\mathrm{days}_{(i)}$ over the number of days in a year is an NPP time correction. Similar to Eq. (5), E_{bio_model} was calculated for the months where $P_{eff(i)} > 0$ only. For a detailed description of EEMT see

HESSD
12, 7933–7969, 2015

Rasmussen et al. (2005, 2011, 2015), Rasmussen and Tabor (2007) and Rasmussen and Gallo (2013).

2.5 Water availability, water partitioning and climate controls on water availability

A trend analysis was conducted using data from 1984 through 2012 on each component of the water partitioning analysis (P, Q, U, S, V, W, Q_{50}), Horton index and EEMT using the nonparametric Mann–Kendall test and the Sen's slope estimator of a linear trend with a $\alpha = 0.10$ level of significance (Yue et al., 2012; Sen, 1968). Relationships between climate, hydrological variables and EEMT were examined by simple and multiple linear regression analysis with parameters fit through a least square iterative process (Haan, 1997).

3 Results

3.1 Climate variability

Records from the Quemazon SNOTEL station from 1984 to 2012 indicated a mean annual precipitation of 701 mm, of which 50 % fell during the winter months with a mean maximum SWE of 242.5 mm. The mean annual and winter temperatures at this site were 3.98 and −0.87 °C, respectively. During the same time period, Señorita Divide#2 station had a mean annual precipitation of 686 mm, of which 61 % fell during the winter with a mean maximum SWE recorded of 239.2 mm. The mean annual and winter temperatures at the Señorita Divide#2 site were 4.23 and −0.90 °C, respectively (Table 2). During the three decades of analysis, seven out of the 13 climate variables in both stations showed a statistically significant trend (Table 3). Mean winter, summer and annual air temperatures at the Quemazon station increased significantly by 1.3, 1.0 and 1.4 °C decade^{-1}, respectively. Similarly, the same variables at the Señorita Divide#2 station

HESSD
12, 7933–7969, 2015

cc BY

increased 1.0, 1.0 and 1.2 °C decade^{-1}, respectively. The rates of increase in winter and annual air temperature were larger in Quemazon, the higher elevation station. Annual precipitation decreased in both stations at similar rates decade^{-1}. Quemazon station decreased 69.8 mm decade^{-1} ($p \leq 0.01$) and Señorita Divide#2 decreased 73.2 mm decade^{-1} ($p \leq 0.05$). Winter precipitation decreased faster at the Señorita Divide #2, the lower elevation station (59.4 mm decade^{-1}; $p \leq 0.05$) than at the Quemazon station (41.6 mm decade^{-1}; $p \leq 0.1$). Maximum SWE decreased in both stations at similar rates, −34.7 mm decade^{-1} at Señorita Divide #2 and −33.1 mm decade^{-1} at the Quemazon station ($p \leq 0.1$). There was no significant trend in the ratio between SWE to winter precipitation at either station. Observed 1 April SWE also decreased −60.5 mm decade^{-1} ($p \leq 0.05$) and −54.4 mm decade^{-1} ($p \leq 0.1$) at the Quemazon and Señorita Divide#2 stations, respectively. The day of occurrence of maximum SWE recorded at the Quemazon station showed a significant trend indicating that maximum SWE is occurring 5.7 days earlier every decade ($p \leq 0.05$). However, this same trend was not observed at the Señorita Divide#2 station. Variables such as SM50, initiation of snow cover, and snow cover duration did not indicate any trend of change in either station at the 90 % confidence level. In contrast, there is a decreasing trend in the last day of snow cover, which is happening about 6 days sooner decade^{-1} in the Quemazon station ($p < 0.05$). Last day of snow cover at the Señorita Divide #2 station did not show a significant trend (Table 3).

3.2 Water partitioning

Mean precipitation in the Jemez River Basin from 1984 to 2012 was 617 mm with observed extreme values of 845 mm in 1985 and 336 mm in 2002. During the analysis period, winter precipitation represented 54 % of total annual precipitation. Mean annual precipitation at the catchment scale correlated significantly with the mean annual precipitation recorded at the Quemazon ($R^2 = 0.45$; $p < 0.0001$) and Señorita Divide#2 stations ($R^2 = 0.73$; $p < 0.0001$). In this same timeframe average, minimum and max-

HESSD
12, 7933–7969, 2015

imum basin scale temperatures were 6.1, −1.5 and 13.6 °C, respectively. In general, January was the coldest and July the warmest month. Basin scale mean annual and winter temperature indicated a statistically significant increasing trend of 0.5 and 0.4 °C decade^{-1} (not shown). Mean annual temperature in the Jemez River Basin significantly correlated with the mean annual temperature recorded at the Quemazon ($R^2 = 0.29$; $p < 0.006$) and Señorita Divide#2 stations ($R^2 = 0.67$; $p < 0.0001$) (not shown). Mean river basin discharge during the study period was 0.15 mm day^{-1} and the maximum and minimum historical streamflow discharges were 2.97 and 0.008 mm day^{-1}, respectively. In the 29 years of daily discharge records, 90 % of the time discharge surpassed 0.03 mm day^{-1} and 10 % of the time exceeded 0.38 mm day^{-1}. Peak discharge occurred between March and May and 58 % of the annual discharge flowed between these months. From 1984 to 2012, three percent of annual precipitation became quickflow and contributed directly to the streamflow discharge (3 % P; standard deviation SD = 1.2 % P). As a result, 97 % of the annual precipitation (SD = 1.2 % P) infiltrated and was available for vegetation uptake. This 97 % of annual precipitation is further partitioned between vaporization and baseflow. The amount of water vaporized into the atmosphere represented 91 % of the annual precipitation (SD = 3.4 % P). Baseflow corresponded to 6.1 % of the annual precipitation (SD = 2.2 % P) and represented the largest component of discharge (73.2 % Q; SD = 5.4 % Q). Quickflow represented the remaining 26.8 % of annual discharge (SD = 5.4 % Q). During the study period, the mean Horton index was 0.94 (SD = 0.02). There was a significant decreasing trend in precipitation and all the water partitioning components in the upper Jemez River Basin as quantified by the Mann–Kendall test (MKT) (Fig. 2). Precipitation in the basin decreased at a rate of −61.7 mm decade^{-1} ($p = 0.02$) (Fig. 2a) while discharge decreased at a rate of −17.6 mm decade^{-1} ($p = 0.001$) (Fig. 2b). The two components of discharge, baseflow and quickflow decreased at a rate of −12.4 mm ($p < 0.001$) and −5.1 mm ($p = 0.005$) decade^{-1}, respectively (Fig. 2c and d). Water loss by vaporization decreased −45.7 mm decade^{-1} ($p = 0.04$; Fig. 2e) and wetting decreased −56.7 mm decade^{-1} ($p < 0.02$; Fig. 2f). As a result, an increasing water limitation trend

HESSD
12, 7933–7969, 2015

was observed in the upper Jemez River Basin as indicated by the decrease in all the water partitioning variables and increase of 0.014 $decade^{-1}$ in the Horton index ($p = 0.002$) (Fig. 2g). In addition to the decreasing trend in the amount of basin scale discharge, Q_{50} showed that 50 % of annual discharge is occurring 4.3 days earlier $decade^{-1}$ ($p = 0.03$).

3.3 EEMT

3.3.1 $EEMT_{emp}$

Using the available 2000 through 2012 remote sensing data, mean MODIS NPP was found to be 450 $g\,C\,m^{-2}$ (SD = 57.1 $g\,C\,m^{-2}$). Using these 13 years of data, no trend in the mean annual NPP for the upper Jemez River Basin was found. However, mean annual NPP was positively correlated with basin scale precipitation ($R^2 = 0.56$; $p = 0.003$) and baseflow ($R^2 = 0.41$; $p = 0.02$) (Fig. 3). These results indicated that forest productivity in the upper Jemez River Basin is primarily limited by water availability since other climate variables recorded at the two SNOTEL stations were not good predictors of NPP. From 1984 through 2012 mean E_{ppt_emp} was 1.03 $MJ\,m^2\,yr^{-1}$ (SD = 0.49 $MJ\,m^2\,yr^{-1}$) and mean E_{bio_emp} was 9.89 $MJ\,m^2\,yr^{-1}$ (SD = 1.26 $MJ\,m^2\,yr^{-1}$). Multivariate regression analysis indicated that precipitation at the Quemazon station and the upper Jemez River Basin were the best predictors of E_{bio_emp} ($R^2 = 0.66$; $p = 0.006$). Using this multivariate linear regression model, E_{bio_emp} data was extrapolated for the years 1984 through 1999. Using the combined dataset from extrapolated and measured E_{bio_emp} the mean annual E_{bio_emp} was 10.8 $MJ\,m^2\,yr^{-1}$ (SD = 1.37 $MJ\,m^2\,yr^{-1}$) for the period from 1984 to 2012. Mean $EEMT_{emp}$ was 11.83 $MJ\,m^2\,yr^{-1}$ (SD = 1.74 $MJ\,m^2\,yr^{-1}$) and E_{bio_emp} represented 92 % (SD = 0.03 %) of the total $EEMT_{emp}$ during the study period.

3.3.2 $EEMT_{model}$

From 1984 through 2012 mean E_{ppt_model} was 0.1 MJ m^2 yr^{-1} (SD = 0.07 MJ m^2 yr^{-1}) and mean E_{bio_model} was 6.72 MJ m^2 yr^{-1} (SD = 2.33 MJ m^2 yr^{-1}). During this same period, mean $EEMT_{model}$ was 6.82 MJ m^2 yr^{-1} (SD = 2.38 MJ m^2 yr^{-1}) and E_{bio_model} represented 99 % (SD = 1.2 %) of the total $EEMT_{model}$.

$EEMT_{emp}$ was on average 1.7 times larger than $EEMT_{model}$. Both $EEMT_{emp}$ and $EEMT_{model}$ showed a significant linear correlation ($R^2 = 0.42$; $p = 0.0002$) and a similar decreasing trend of 1.2 MJ m^2 decade^{-1} ($p \leq 0.01$) and 1.3 MJ m^2 decade^{-1} ($p \leq 0.05$), respectively (Fig. 4). Detailed estimations of $EEMT_{emp}$ and $EEMT_{model}$ and its components can be found in Table S1 (Supplement). Figure 5 highlights changes of EEMT in the upper Jemez River Basin in relation to water availability from 1984 to 2012. EEMT was positively correlated to annual baseflow, increasing during wet years and decreasing during dry years.

3.4 Climate controls on discharge

When compared to the climate variables from the Quemazon station, data from the Señorita Divide#2 showed the strongest linear correlations with discharge (Table S2). The five variables with the strongest linear correlations to discharge were winter precipitation ($R^2 = 0.72$; $p = 0.00001$), maximum SWE ($R^2 = 0.55$; $p = 0.00001$), last day of snow cover ($R^2 = 0.54$; $p = 0.00001$), annual precipitation ($R^2 = 0.50$; $p = 0.00001$), and annual temperature ($R^2 = 0.49$; $p = 0.00010$). Variables such as first day of snow cover, SWE to winter P ratio and SM50 did not shown any relation.

Similarly, climate variables from Señorita Divide#2 showed the strongest linear correlations with Horton index (Table S3). The five variables with the strongest linear correlations to Horton index were winter precipitation ($R^2 = 0.59$; $p = 0.00001$), maximum SWE ($R^2 = 0.59$; $p = 0.00001$), last day of snow cover ($R^2 = 0.55$; $p = 0.00001$), occurrence of 50 % max SWE ($R^2 = 0.41$; $p = 0.00010$), and annual temperature ($R^2 = 0.40$;

HESSD
12, 7933–7969, 2015

CC BY

$p = 0.00070$). SM50 was the only variable that did not show a strong linear correlation with Horton index at the Señorita Divide#2 station.

Based on a multivariate regression analysis, annual temperature, max SWE and the length of snow on the ground were the best predictors of discharge and explain above 80 % of discharge variability in the basin ($R^2 > 0.80$; $p < 0.0001$) (Table 4). The predictive power of this model was similar regardless of whether data from the Quemazon or Señorita Divide#2 stations was used. From these three predicting variables, annual temperature and max SWE showed decreasing trends that influence the observed decrease in water availability in the basin. Analysis of residuals of the linear model between climate variables and Jemez River discharge indicated that maximum SWE and the duration of the snow cover are the better predictors of discharge residuals variability. As it is shown in Fig. S1, Q residuals increased during extreme dry and wet years.

4 Discussion

4.1 Climate variability

Global climate is changing and the instrumental records in the southwestern US for the last three decades indicate a decline in precipitation and increasing air temperatures in the region (Hughes and Diaz, 2008; Folland et al., 2001). Global climate models further predict drier conditions and a more arid climate for the 21st century in this region (Seager et al., 2007). For instance, global climate models indicate, for the future in the southwestern US according to a low and high emissions scenarios, a substantial increase in air temperature between 0.6 to 2.2 °C and 1.3 to 5.0 °C for the period 2021–2050 and by end of the 21st century, respectively (Barnett et al., 2004; Cayan et al., 2013). An increase in winter temperature of about 0.6 °C decade^{-1} was reported from 1984–2012 at a regional level in the upper Rio Grande Basin (Harpold et al., 2012). In

HESSD
12, 7933–7969, 2015

CC BY

line with these other studies, we found that mean annual and winter air temperature in the upper Jemez River Basin have increased 0.5 and 0.4 °C decade^{-1}, respectively.

Changes in climate have been found to be a predominant influence in snowpack decline as oppose to changes in land use, forest canopy or other factors (Hamlet et al., 2005; Boisvenue and Running, 2006). There are high confidence predictions that snowpacks will continue to decline in northern New Mexico through the year 2100 and projections of snowpack accumulation for mid-century (2041–2070) show a marked reduction for SWE of about 40 % (Cayan et al., 2013). Harpold et al. (2012) found a decrease in annual precipitation and maximum SWE for the Upper Rio Grande Basin of −33 and −40 mm decade^{-1}, respectively. In this study, a clear decreasing trend in annual, winter precipitation and max SWE was observed in records from 1984–2012 in the two high elevation SNOTEL stations. Records in this study showed approximately twice the rate of decrease in annual precipitation and a smaller decrease in max SWE of about 7 mm decade^{-1} compared to the regional results from Harpold et al. (2012). Harpold et al. (2012) report that SM50 (−2 days decade^{-1}), snow cover length (−4.2 days decade^{-1}), day of maximum SWE (−3.31 days decade^{-1}), and last day of snow cover (−3.45 days decade^{-1}) for the Rio Grande Basin showed statistically significant trends. However, based on our analysis from the individual SNOTEL stations, these variables did not show any statistically significant trends.

4.2 Changes in discharge and evapotranspiration

Decreasing trends in discharge ranging from 10 to 30 % are expected during the 21st century for the western US (Milly et al., 2005) and maximum peak streamflow is expected to happen one month earlier by 2050 (Barnett et al., 2005). Furthermore, it has been reported that streamflow in snowmelt dominated river basins are more sensitive to wintertime increases in temperature (Barnett et al., 2005). In this study, we have found that 50.5 % of annual streamflow occurred between (April) and beginning of the summer (June). This result is congruent with other studies in snowmelt dominated systems in the region (Clow, 2010). Previous research in the southwest has found that the

HESSD
12, 7933–7969, 2015

cc BY

timing of snowmelt is shifting to early times ranging from a few days to weeks (Stewart et al., 2004; Mote et al., 2005; McCabe and Clark, 2005). For instance, Clow (2010) reports that in southern Colorado rivers, there is a trend toward earlier snowmelt that varied from 4.0 to 5.9 days $decade^{-1}$ and 1 April SWE decreased between 51 and 95 mm $decade^{-1}$. In this study, it was found that snowmelt timing in the upper Jemez River Basin occurred 4.3 days earlier $decade^{-1}$ and 1 April SWE decreased between 54–60 mm $decade^{-1}$.

Changes in evapotranspiration are related to changes in precipitation, humidity, air temperature, irradiance and wind speed (Barnet et al., 2005). However, the magnitude and direction of changes in evapotranspiration are still a source of debate and investigation (Ohmura and Wild, 2002). Pan evaporation in various countries in the Northern Hemisphere show that evaporation has been progressively decreasing over the past 50 years (Barnett et al., 2005). A reduction in evapotranspiration is expected in snowmelt dominated systems, as early snowmelt provides water to the landscape when potential evapotranspiration is low and reducing soil moisture during months with high evapotranspiration demand (Barnett et al., 2005). In addition, rising CO_2 concentrations will likely increase plant water use efficiency, enhance stomatal closure and reduce transpiration (Betts et al., 2005). In this study, we found evidence of a decrease in vaporization of 45.7 mm $decade^{-1}$ in the upper Jemez River basin.

4.3 EEMT components

4.3.1 Water partitioning

Troch et al. (2009) demonstrated that the Horton index gets closer to 1 in drier regions and during dry years. Similarly, in a study based on 86 catchments in different biomes and ecosystems across the US, Horton index values increased as catchments became more water limited (Brooks et al., 2011). Huxman et al. (2004) showed that the average rain-use efficiency (RUE), estimated as the ratio of aboveground net primary production to annual precipitation, decreases as precipitation increases. In contrast, during

cc BY

dry years RUE converges to common maximum RUE similar to the drier regions, regardless of biome type. The increase in water use efficiency by vegetation as the upper Jemez River basin becomes drier indicated by the Horton index variability (0.94; SD = 0.02) is consistent with the above mentioned studies.

4.3.2 Forest productivity

Reduced carbon compounds resulting from primary production are a fundamental energy component of EEMT (Rasmussen et al., 2011). Modeling and empirical studies indicate that mountain forest productivity in the southwest is sensitive to water and energy limitations (Christensen et al., 2008; Tague et al., 2009; Anderson-Teixeira et al., 2011; Zapata-Rios et al., 2015b; Zapata-Rios, 2015). Trujillo et al. (2012) found that NDVI greening increased and decreased proportionally to the changes in snowpack accumulation along a gradient in elevation in the Sierra Nevada, while Zapata-Rios et al. (2015b); Zapata-Rios (2015) found similar results across a gradient of energy created by aspect differences at higher elevations in the Jemez Mountains. Furthermore, energy limitations to productivity have been observed in colder sites at high elevations (Trujillo et al., 2012; Anderson-Teixeira et al., 2011; Zapata-Rios et al. 2015b; Zapata-Rios, 2015). Since the mid-1980 increases in wildfires and tree mortality rates have been documented in high elevation forests due to an increase in spring and summer temperatures and decrease in water availability (Westerling et al., 2006; Van Mantgem et al., 2009). Results from this study indicated that in the upper Jemez River Basin, forest productivity was primarily responding to water availability (Fig. 3).

4.4 EEMT variability

All of the above results indicate that the Jemez River Basin is highly susceptible to changes in climate that can affect water availability and ecosystem productivity which impacts EEMT. Rasmussen et al. (2005) estimated low rates of $\mathrm{EEMT_{model}} < 15$ $\mathrm{MJ\,m^{-2}\,yr^{-1}}$ for the majority of the continental US and demonstrated that E_{bio} was the

HESSD
12, 7933–7969, 2015

dominant component of EEMT with contributions above 50 % of total EEMT in soil orders associated with arid and semiarid regions. Regions dominated by E_{bio} corresponded to regions facing water limitation and where E_{bio} accounted for up to 93 % of the total energy and carbon flux to the CZ (Rasmussen et al., 2011; Rasmussen and Gallo, 2013). In semi-arid regions vaporization represents over 90 % loss of annual precipitation (Newman et al., 2006) while groundwater recharge accounts for less than 10 % of annual precipitation (Scanlon et al., 2006). Under these conditions, little water remains for critical zone processes in semi-arid regions. Other studies have found that the contributions of E_{bio} can be three to seven orders of magnitude larger than other sources of energy influxes to the CZ (Phillips, 2009; Amundson et al., 2007). In this study, we confirmed that for the upper Jemez River Basin, E_{bio} was the dominant term from the total EEMT and E_{ppt} contributions were small.

A comparison of $EEMT_{model}$ and $EEMT_{emp}$ in 86 catchments across the US characterized by having minimum snow influence indicated that model and empirical values were strongly linearly correlated ($R^2 = 0.75$; $p < 0.0001$) and $EEMT_{model}$ values were larger than $EEMT_{emp}$ (Rasmussen and Gallo, 2013). One limitation of the $EEMT_{model}$ method is that it calculates energy during the months when air temperature is above zero only and assumes no energy associated with precipitation falling as snow. In a snowmelt dominated systems as the upper Jemez River Basin where snowmelt is the main source of water availability to ecosystems (Bales et al., 2006), EEMT estimations based only on climate data will likely underestimate the energy transfer to the CZ. Therefore, using $EEMT_{emp}$ methodology may be more suitable for snowmelt dominated systems. In this study we found the expected linear correlation between $EEMT_{model}$ and $EEMT_{emp}$ ($R^2 = 0.42$; $p < 0.001$) however, $EEMT_{model}$ values were smaller than $EEMT_{emp}$ values. Although the two methods used in this study to calculate EEMT indicated different absolute values of EEMT, the rates of decrease of EEMT decade^{-1} are congruent with each other ($EEMT_{emp} = 1.2$ MJ m^2 decade^{-1}; $EEMT_{model} = 1.3$ MJ m^2 decade^{-1}) (Fig. 5).

The rates of EEMT change found in this study between 1.2 to 1.3 $\mathrm{MJ\,m^2\,decade^{-1}}$ in the upper Jemez River Basin can be significant for critical zone processes. Over long time scales this change could represent an upward movement of more arid, lower EEMT systems to higher elevations. For instance, in a study conducted in a similar semi-arid region in the Santa Catalina Mountains (SCM) located in southern Arizona, Rasmussen et al. (2015) estimated differences in EEMT of about 25 $\mathrm{MJ\,m^2\,yr^{-1}}$ between the upper elevation (2800 m) covered by mixed conifer forest and low elevation (800 m) covered by a dry semi-arid desert scrub ecosystem. These changes in EEMT along the 2000 m elevation gradient in the SCM are equivalent to a difference of 1.25 $\mathrm{MJ\,m^2\,yr^{-1}}$ per 100 m in elevation change. Along this elevation gradient contrasting soil characteristics, regolith development, chemical depletion and mineral transformation have been observed between lower and high elevations on similar granitic parent material (Lybrand et al., 2011; Lybrand and Rasmussen, 2014). Molisols and carbon rich soils have been characterized in convergent areas of greater EEMT vs. weakly developed Entisols in lower EEMT landscape positions (Lybrand et al., 2011; Holleran et al., 2015). Furthermore, Rasmussen et al. (2015) determined differences of 3.9 $\mathrm{MJ\,m^2\,yr^{-1}}$ between contrasting north and south facing slopes at a similar elevation. In areas with similar EEMT north facing slopes have soils characterized by greater clay and carbon accumulation (Holleran et al., 2015). According to topographic wetness differences of 0.9 $\mathrm{MJ\,m^2\,yr^{-1}}$ were determined between water gaining and water losing portions of the landscape (Rasmussen et al., 2015).

Although the quantification of EEMT using the methodologies applied in this study are suitable for large spatial scales, it is limited in that it is not taking into account small scale variabilities induced by topography in solar energy, effective precipitation, NPP and redistribution of water by differences in micro-topography. Therefore, EEMT estimations at small scales (pedon to hillslopes) need to follow a different approach as indicated in Rasmussen et al. (2015).

Discussion Paper | Discussion Paper | Discussion Paper | Discussion Paper |

CC BY

5 Summary

We investigated how changes in climate in the southwest affect the trends in water availability, vegetation productivity and the annual influxes of EEMT to the CZ. This investigation took place in the 1200 km^2 upper Jemez River basin a semi-arid basin in northern New Mexico using records from 1984–2012. Results at the two SNOTEL stations indicated clear increasing trends in temperature and decreasing trends in precipitation and maximum SWE. Temperature changes include warmer winters (+1.0–1.3 °C $decade^{-1}$), and generally warmer year round temperatures (+1.2–1.4 °C $decade^{-1}$). Precipitation changes include, a decreasing trend in precipitation during the winter (−41.6–51.4 mm $decade^{-1}$), during the year (−69.8–73.2 mm $decade^{-1}$) and max SWE (−33.1–34.7 mm $decade^{-1}$). At the upper Jemez River Basin, all the water partitioning components showed statistical significant decreasing trends including precipitation (−61.7 mm $decade^{-1}$), discharge (−17.6 mm $decade^{-1}$) and vaporization (−45.7 mm $decade^{-1}$). Similarly, Q_{50} an indicator of snowmelt timing is occurring −4.3 days $decade^{-1}$ earlier. Basin scale precipitation ($R^2 = 0.56$; $p = 0.003$) and baseflow ($R^2 = 0.41$; $p = 0.02$) were the strongest controls on NPP variability indicating that forest productivity in the upper Jemez River Basin is water limited. An increasing trend in Horton index suggests that water limitation and vegetation water use are increasing in the basin. This study showed a positive correlation between water availability and EEMT. For every 10 mm of change in baseflow, EEMT varies proportionally in 0.6–0.7 MJ m^{-2} yr^{-1}. From 1984–2012 changes in climate, water availability, and NPP have influenced EEMT in the upper Jemez River Basin. A decreasing trend in EEMT of 1.2 to 1.3 MJ m^{-2} $decade^{-1}$ was calculated in this same time frame. As the landscape moves towards a drier and hotter climate, changes in EEMT of this magnitude are likely to influence critical zone processes.

The Supplement related to this article is available online at doi:10.5194/hessd-12-7933-2015-supplement.

HESSD

12, 7933–7969, 2015

Author contributions. All authors contributed extensively to this research. All authors discussed the methodology, results and commented on the manuscript at all stages. X. Zapata-Rios analyzed data and prepared the manuscript with contributions from all co-authors.

Acknowledgements. We thank the funding provided by the NSF-supported Jemez River Basin and Santa Catalina Mountains Critical Zone Observatory EAR-0724958 and EAR-1331408.

References

Allen, C., Savage, M., Falk, D., Suckling, K., Swetnam, T., Schulke, T., Stacey, P., Morgan, P., Hoffman, M., and Klingel, J.: Ecological restoration of Southwestern ponderosa pine ecosystems: a broad perspective, Ecol. Appl., 12, 1418–1433, 2002.

Allen, R., Peet, R., and Baker, W.: Gradient analysis of latitudinal variation in Southern Rocky-Mountain Forests, J. Biogeogr., 18, 123–139, 1991.

Amundson, R., Richter, D. D., Humphreys, G. S., Jobbagy, E. G., and Gaillardet, J.: Coupling between biota and earth materials in the critical zone, Elements, 3, 327–332, 2007.

Anderson, S. P., von Blanckenburg, F., and White, A. F.: Physical and chemical controls on the critical zone, Elements, 3, 315–319, 2007.

Anderson-Teixeira, K. J., Delong, J. P., Fox, A. M., Brese, D. A., and Litvak, M. E.: Differential responses of production and respiration to temperature and moisture drive the carbon balance across a climatic gradient in New Mexico, Glob. Change Biol., 17, 410–424, 2011.

Arnold, J. and Allen, P.: Automated methods for estimating baseflow and ground water recharge from streamflow records, J. Am. Water Resour. As., 35, 411–424, 1999.

Bales, R. C., Molotch, N. P., Painter, T. H., Dettinger, M. D., Rice, R., and Dozier, J.: Mountain hydrology of the western United States, Water Resour. Res., 42, W08432, 2006.

Barnett, T., Malone, R., Pennell, W., Stammer, D., Semtner, B., and Washington, W.: The effects of climate change on water resources in the west: introduction and overview, Climatic Change, 62, 1–11, 2004.

Barnett, T., Adam, J., and Lettenmaier, D.: Potential impacts of a warming climate on water availability in snow-dominated regions, Nature, 438, 303–309, 2005.

Betts, R. A., Boucher, O., Collins, M., Cox, P. M., Falloon, P. D., Gedney, N., Hemming, D. L., Huntingford, C., Jones, C. D., Sexton, D. M. H., and Webb, M. J.: Projected increase in

CC BY

continental runoff due to plant responses to increasing carbon dioxide, Nature, 448, 1037, 2007.

Boisvenue, C. and Running, S.: Impacts of climate change on natural forest productivity – evidence since the middle of the 20th century, Glob. Change Biol., 12, 862–882, 2006.

Brantley, S. L., Goldhaber, M. B., and Ragnarsdottir, K. V.: Crossing disciplines and scales to understand the Critical Zone, Elements, 3, 307–314, 2007.

Brooks, P. D., Troch, P. A., Durcik, M., Gallo, E., and Schlegel, M.: Quantifying regional scale ecosystem response to changes in precipitation: not all rain is created equal, Water Resour. Res., 47, W00J08, doi:10.1029/2010WR009762, 2011.

Cayan, D., Tyree, M., Kunkel, K. E., Castro, C., Gershunov, A., Barsugli, J., Ray, A. J., Overpeck, J., Anderson, M., Russell, J., Rajagopalan, B., Rangwala, I., and Duffy, P.: Future Climate: Projected Average, in: Assessment of Climate Change in the Southwest United States: A Report Prepared for the National Climate Assessment, edited by: Garfin, G., Jardine, A., Merideth, R., Black, M., and LeRoy, S., Island Press, Washington, DC, 101–125, 2013.

Chorover, J., Troch, P. A., Rasmussen, C., Brooks, P. D., Pelletier, J. D., Breshears, D. D., Huxman, T. E., Kurc, S. A., Lohse, K. A., McIntosh, J. C., Meixner, T., Schaap, M. G., Litvak, M. E., Perdrial, J., Harpold, A., and Durcik, M.: How water, carbon, and energy drive critical zone evolution: the Jemez-Santa Catalina critical zone observatory, Vadose Zone J., 10, 884–899, 2011.

Christensen, L., Tague, C. L., and Baron, J. S.: Spatial patterns of simulated transpiration response to climate variability in a snow dominated mountain ecosystem, Hydrol. Process., 22, 3576–3588, 2008.

Clow, D. W.: Changes in the timing of snowmelt and streamflow in Colorado: a response to recent warming, J. Climate, 23, 2293–2306, 2010.

Daly, C., Gibson, W., Taylor, G., Johnson, G., and Pasteris, P.: A knowledge-based approach to the statistical mapping of climate, Clim. Res., 22, 99–113, 2002.

Eckhardt, K.: How to construct recursive digital filters for baseflow separation, Hydrol. Process., 19, 507–515, 2005.

Folland, C. K., Karl, T. R., Christy, J. R., Clarke, R. A., Gruza, G. V., Jouzel, J., Mann, M. E., Oerlemans, J., Salinger, M. J. and Wange, S. W.: Observe climate variability and change, in: Climate Change 2001: the Scientific Basis, Contribution of working group I to the third Assessment Report of the Intergovernmental Panel on Climate Change, edited by: Houghton, J. T.,

HESSD
12, 7933–7969, 2015

CC BY

Ding, Y., Griggs, D. J., Noguer, M., van der Linden, P. J., Dai, X., Maskell, K., and Johnson, C. A., Cambridge University Press, Cambridge, UK, 99–181, 2001.

Haan, C. T.: Statistical Methods in Hydrology, The Iowa State University Press, Ames, Iowa, 378 pp., 1977.

Hamlet, A., Mote, P., Clark, M., and Lettenmaier, D.: Effects of temperature and precipitation variability on snowpack trends in the western United States, J. Climate, 18, 4545–4561, 2005.

Harpold, A., Brooks, P., Rajagopal, S., Heidbuchel, I., Jardine, A., and Stielstra, C.: Changes in snowpack accumulation and ablation in the intermountain west, Water Resour. Res., 48, W11501, 2012.

Holleran, M., Levi, M., and Rasmussen, C.: Quantifying soil and critical zone variability in a forested catchment through digital soil mapping, Soil, 1, 47–64, doi:10.5194/soil-1-47-2015, 2015.

Hughes, M. K. and Diaz, H. F.: Climate variability and change in the drylands of Western North America, Global Planet. Change, 64, 111–118, 2008.

Huxman, T., Smith, M., Fay, P., Knapp, A., Shaw, M., Loik, M., Smith, S., Tissue, D., Zak, J., Weltzin, J., Pockman, W., Sala, O., Haddad, B., Harte, J., Koch, G., Schwinning, S., Small, E., and Williams, D.: Convergence across biomes to a common rain-use efficiency, Nature, 429, 651–654, 2004.

Lieth, H.: Modeling the primary productivity of the world, in: Primary Productivity of the Biosphere, edited by: Lieth, H. and Whittaker, R. H., Springer-Verlag, New York, p. 237–263, 1975.

Lybrand, R. A. and C. Rasmussen.: Linking soil element-mass-transfer to microscale mineral weathering across a semiarid environmental gradient, Chem. Geol., 381, 26–39, 2014.

Lybrand, R. A., Rasmussen, C., Jardine, A., Troch, P. A., and Chorover, J.: The effects of climate and landscape position on chemical denudation and mineral transformation in the Santa Catalina mountain critical zone observatory, Appl. Geochem., 26, S80–S84, 2011.

Lyne, V. and Hollick, M.: Stochastic time-variable rainfall–runoff modelling, in: Hydrol. And Water Resources. Syp., publ. 79/10, Inst. Eng. Austr. Natl. Conf., Perth, Australia, 89–92, 1979.

McCabe, G. and Clark, M.: Trends and variability in snowmelt runoff in the western United States, J. Hydrometeorol., 6, 476–482, 2005.

Milly, P., Dunne, K., and Vecchia, A.: Global pattern of trends in streamflow and water availability in a changing climate, Nature, 438, 347–350, 2005.

HESSD

12, 7933–7969, 2015

Influence of climate variability on EEMT in a semi-arid critical zone

X. Zapata-Rios et al.

CC BY

Mote, P., Hamlet, A., Clark, M., and Lettenmaier, D.: Declining mountain snowpack in western north America, B. Am. Meteorol. Soc., 86, doi:10.1175/BAMS-86-1-39, 2005.
Nayak, A., Marks, D., Chandler, D. G., and Seyfried, M.: Long-term snow, climate, and streamflow trends at the Reynolds Creek Experimental Watershed, Owyhee Mountains, Idaho, United States, Water Resour. Res., 46, W06519, doi:10.1029/2008WR007525, 2010.
Newman, B. D., Wilcox, B. P., Archer, S. R., Breshears, D. D., Dahm, C. N., Duffy, C. J., McDowell, N. G., Phillips, F. M., Scanlon, B. R., and Vivoni, E. R.: Ecohydrology of water-limited environments: a scientific vision, Water Resour. Res., 42, W06302, doi:10.1029/2005WR004141, 2006.
Ohmura, A. and Wild, M.: Is the hydrological cycle accelerating?, Science, 298, 1345–1346, 2002.
Pelletier, J. D. and Rasmussen, C.: Geomorphically based predictive mapping of soil thickness in upland watersheds, Water Resour. Res., 45, W09417, doi:10.1029/2008WR007319, 2009a.
Pelletier, J. D. and Rasmussen, C.: Quantifying the climatic and tectonic controls on hillslope steepness and erosion rate, Lithosphere, 1, 73–80, 2009b.
Pelletier, J. D., Barron-Gafford, G. A., Breshears, D. D., Brooks, P. D., Chorover, J., Durcik, M., Harman, C. J., Huxman, T. E., Lohse, K. A., Lybrand, R., Meixner, T., McIntosh, J. C., Papuga, S. A., Rasmussen, C., Schaap, M., Swetnam, T. L., and Troch, P. A.: Coevolution of nonlinear trends in vegetation, soils, and topography with elevation and slope aspect: a case study in the sky islands of southern Arizona, J. Geophys. Res.-Earth, 118, 741–758, 2013.
Phillips, J. D.: Biological energy in landscape evolution, Am. J. Sci., 309, 271–289, 2009.
Rasmussen, C.: Thermodynamic constraints on effective energy and mass transfer and catchment function, Hydrol. Earth Syst. Sci., 16, 725–739, doi:10.5194/hess-16-725-2012, 2012.
Rasmussen, C. and Gallo, E. L.: Technical Note: A comparison of model and empirical measures of catchment-scale effective energy and mass transfer, Hydrol. Earth Syst. Sci., 17, 3389–3395, doi:10.5194/hess-17-3389-2013, 2013.
Rasmussen, C. and Tabor, N. J.: Applying a quantitative pedogenic energy model across a range of environmental gradients, Soil Sci. Soc. Am. J., 71, 1719–1729, 2007.
Rasmussen, C., Southard, R., and Horwath, W.: Modeling energy inputs to predict pedogenic environments using regional environmental databases, Soil Sci. Soc. Am. J., 69, 1266–1274, 2005.

HESSD
12, 7933–7969, 2015
Influence of climate variability on EEMT in a semi-arid critical zone
X. Zapata-Rios et al.

Rasmussen, C., Troch, P. A., Chorover, J., Brooks, P., Pelletier, J., and Huxman, T. E.: An open system framework for integrating critical zone structure and function, Biogeochemistry, 102, 15–29, 2011.
Rasmussen, C., Pelletier, J. D., Troch, P. A., Swetnam, T. L., and Chorover, J..: Quantifying topographic and vegetation effects on the transfer of energy and mass to the critical zone, Vadose Zone J., doi:10.2136/vzj2014.07.0102, 2015.
Scanlon, B. R., Keese, K. E., Flint, A. L., Flint, L. E., Gaye, C. B., Edmunds, W. M., and Simmers, I.: Global synthesis of groundwater recharge in semiarid and arid regions, Hydrol. Process., 20, 3335–3370, 2006.
Seager, R., Ting, M., Held, I., Kushnir, Y., Lu, J., Vecchi, G., Huang, H., Harnik, N., Leetmaa, A., Lau, N., Li, C., Velez, J., and Naik, N.: Model projections of an imminent transition to a more arid climate in southwestern North America, Science, 316, 1181–1184, 2007.
Sen, P. K.: Estimates of the regression coefficient based on Kendall's tau, J. Am. Stat. Assoc., 63, 1379–1389, 1968.
Sheppard, P., Comrie, A., Packin, G., Angersbach, K., and Hughes, M.: The climate of the US Southwest, Clim. Res., 21, 219–238, 2002.
Shevenell, L., Goff, F., Vuataz, F., Trujillo, P. E., Counce, D., Janik, C. and Evans, W.: Hydrogeochemical data for thermal and nonthermal waters and gases of the Valles Caldera – Southern Jemez Mountains Region, New Mexico, Technical report, Los Alamos National Lab, Los Alamos, New Mexico, N M.LA-10923-OBES, 1987.
Steffen, W., Crutzen, P. J., and McNeill, J. R.: The anthropocene: are humans now overwhelming the great forces of nature, Ambio, 36, 614–621, 2007.
Stewart, I., Cayan, D., and Dettinger, M.: Changes in snowmelt runoff timing in western North America under a "business as usual" climate change scenario, Climatic Change, 62, 217–232, 2004.
Tague, C., Heyn, K., and Christensen, L.: Topographic controls on spatial patterns of conifer transpiration and net primary productivity under climate warming in mountain ecosystems, Ecohydrology, 2, 541–554, 2009.
Thornthwaite, C. W.: An approach toward a rational classification of climate, Geogr. Rev., 38, 55–94, 1948.
Troch, P. A., Martinez, G. F., Pauwels, V. R. N., Durcik, M., Sivapalan, M., Harman, C., Brooks, P. D., Gupta, H., and Huxman, T.: Climate and vegetation water use efficiency at catchment scales, Hydrol. Process., 23, 2409–2414, 2009.

CC BY

Trujillo, E., Molotch, N. P., Goulden, M. L., Kelly, A. E., and Bales, R. C.: Elevation-dependent influence of snow accumulation on forest greening, Nat. Geosci., 5, 705–709, 2012.
van Mantgem, P. J., Stephenson, N. L., Byrne, J. C., Daniels, L. D., Franklin, J. F., Fule, P. Z., Harmon, M. E., Larson, A. J., Smith, J. M., Taylor, A. H., and Veblen, T. T.: Widespread increase of tree mortality rates in the western united states, Science, 323, 521–524, 2009.
Voepel, H., Ruddell, B., Schumer, R., Troch, P. A., Brooks, P. D., Neal, A., Durcik, M., and Sivapalan, M.: Quantifying the role of climate and landscape characteristics on hydrologic partitioning and vegetation response, Water Resour. Res., 47, W00J09, doi:10.1029/2010WR009944, 2011.
Westerling, A. L., Hidalgo, H. G., Cayan, D. R., and Swetnam, T. W.: Warming and earlier spring increase western US forest wildfire activity, Science, 313, 940–943, 2006.
Yue, S., Pilon, P., and Cavadias, G.: Power of the Mann–Kendall and Spearman's rho tests for detecting monotonic trends in hydrological series, J. Hydrol., 259, 254–271, 2002.
Zapata-Rios, X.: The influence of climate and landscape on hydrological processes, vegetation dynamics, biogeochemistry and the transfer of effective energy and mass to the critical zone, PhD Dissertation, Univ. of Ariz., Tucson, Arizona., 192 pp., 2015.
Zapata-Rios, X., McIntosh, J. Rademacher, L., Troch, P. A., Brooks, P. D., Rasmussen, C., and Chorover J.: Climatic and landscape controls on water transit times and silicate mineral weathering in the critical zone, Water Resour. Res., 51, doi:10.1002/2015WR017018, 2015a.
Zapata-Rios, X.,Troch, P. A., Brooks, P. D., and McIntosh, J.: Influence of terrain aspect on water partitioning, vegetation structure, and vegetation greening in high elevation catchments in northern New Mexico, Ecohydrology, accepted, 2015b.
Zhao, M. and Running, S. W.: Drought-induced reduction in global terrestrial net primary production from 2000 through 2009, Science, 329, 940–943, 2010.

Discussion Paper | Discussion Paper | Discussion Paper | Discussion Paper |

HESSD
12, 7933–7969, 2015

Table 1. Land use classification of the Jemez River Basin area. 79.7 % of the total basin is covered by forest according to the National Land Cover Database (NLCD) http://www.mrlc.gov/nlcd06_leg.php.

Land use class	Area (km^2)	%
Evergreen forest	847.7	69.60
Deciduous forest	92.6	7.61
Mixed forest	29.8	2.44
Grassland/herbaceous	128.0	10.51
Shrub/scrub	85.0	6.98
Pasture/Hay	1.8	0.14
Barren land (rock, sand, clay)	1.3	0.10
Developed	6.1	0.50
Cultivated crops	0.1	0.01
Wetlands	25.2	2.07
Open water	0.4	0.03
Total	1218.0	100.00

HESSD
12, 7933–7969, 2015

CC BY

Table 2. Site and meteorological information for the SNOTEL Quemazon and Señorita Divide #2 stations located at high elevations in the upper part of the Jemez River Basin.

Station Id	Station Name	Elevation (m)	Latitude (N)	Longitude (W)	Active since	Mean Air Temperature (°C)		Mean Precipitation (mm)		Max SWE (mm)
						Year[a]	Winter[b]	Year[a]	Winter[b]	
708	Quemazon	2896	35.92°	−106.39°	1980	3.98	−0.87	700.78	347.45	242.53
744	Senorita Divide #2	2622	36.00°	−106.83°	1980	4.23	−0.90	685.98	422.87	239.20

Note:
The analysis of precipitation since WY 1984.
[a]Water Year: 1 October to 30 September
[b] Winter: 1 October to 31 March
Temperature data availability since 1989 for the Quemazon and 1988 for the Senorita Divide #2 station.

HESSD
12, 7933–7969, 2015

Table 3. Climatic time series trends for the Quemazon and Señorita Divide #2 SNOTEL stations from 1984–2012. A trend in the precipitation time series was evaluated with the Mann–Kendall test (MKT) and Sen's slope estimator. Trends were considered statistically significant at $p \leq 0.1$. The results showed an increasing trend in winter, summer and annual temperature in the two stations. Annual and winter precipitation, maximum SWE and 1 April SWE decreased in both stations during the 29 years analyzed. The last day of snow cover decreases significantly only at the Quemazon station. No significant trend was observed for the SWE: winter P ratio, duration of snowmelt SM50 and length of snow on the ground.

Variable	Quemazon Q Sen's slope estimator	Sig [a]	Señorita Divide #2 Q Sen's slope estimator	Sig [a]
Winter Temp	0.13	****	0.10	**
Summer Temp	0.10	***	0.10	***
Annual temp	0.14	****	0.12	****
Annual Precip(mm)	−6.98	***	−7.32	**
Winter Precip (mm)	−4.16	*	−5.94	**
Max SWE (mm)	−3.31	*	−3.47	*
SWE:winter P ratio	−0.005		−0.002	
1 Apr SWE	−6.05	**	−5.44	*
Max SWE day	−0.57	**	−0.33	
SM50 (days)	−0.02		0.12	
1st day snow cover (day)	−0.50		0.17	
last day snow cover (day)	−0.65	**	−0.31	
snow on ground (days)	−0.12		−0.60	

[a] Statistical significance
[*] $P < 0.1$
[**] $P < 0.05$
[***] $P < 0.01$
[****] $P < 0.001$

HESSD
12, 7933–7969, 2015

Table 4. Discharge predictors for the Jemez River basin based on climate variables recorded at Quemazon and Señorita Divide#2 SNOTEL stations. Annual temperature, max SWE and the length of snow on the ground were the best predictors of discharge in the basin. The predictability power of discharge was similar from climatic variables recorded at the Quemazon and Señorita Divide#2 stations. Annual temperature and max SWE climatic variables had a decreasing trend that influenced the decrease in water availability in the basin.

	Quemazon		Señorita Divide#2	
		p values		p values
Intercept	−7.57	0.071	37.75	0.0128
Annual Temp (°C)	−7.23	0.0035	−3.5	0.07
Max SWE (mm)	0.14	0.0003	0.21	0.0001
Snow on the ground (days)	0.32	0.03	−0.18	0.05
R^2	0.81		0.80	
p	< 0.0001		< 0.0001	

HESSD
12, 7933–7969, 2015

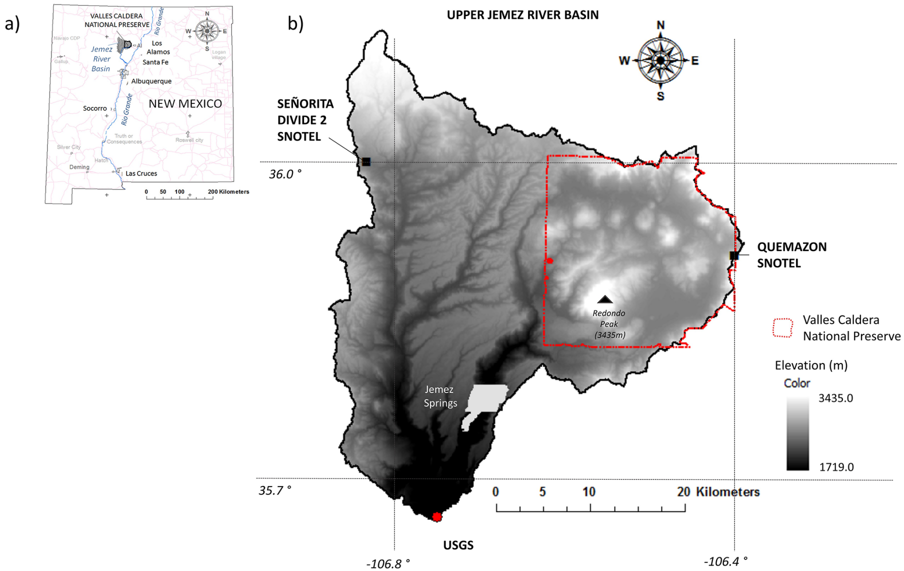

Figure 1. (a) Relative location of study area within the northwestern state of New Mexico, **(b)** upper Jemez River Basin, ∼ 1200 km^2, delimited above the USGS gauge station "Jemez River near Jemez" (USGS 08324000) based on a 10 m digital elevation model (DEM).

HESSD
12, 7933–7969, 2015

CC BY

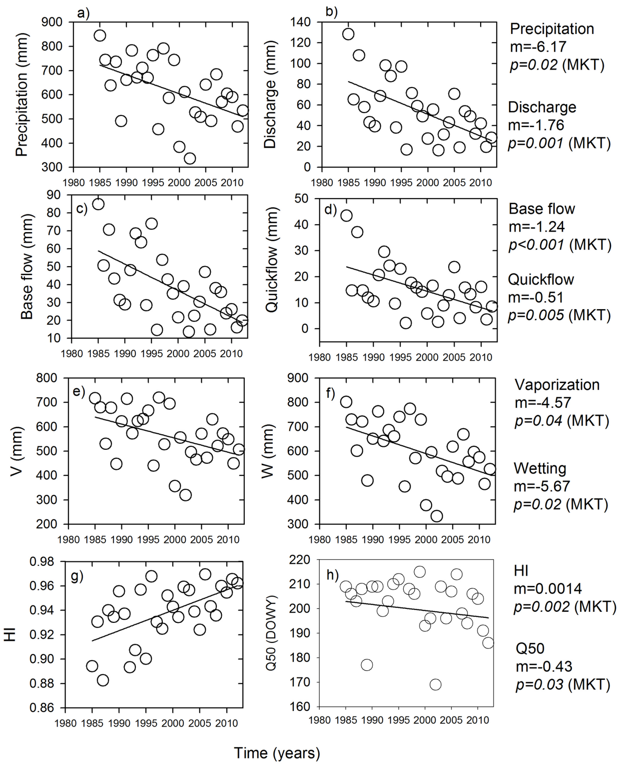

Figure 2. Precipitation and water partitioning at the upper Jemez River catchment scale. There was a significant decreasing trend quantified by the Mann–Kendall test (MKT) in the Jemez River Basin precipitation and all the components of the water partitioning. For instance, precipitation at the catchment scale decreased during the last three decades at a rate of 6.17 mm yr^{-1} and discharge at 1.76 mm yr^{-1}. From 1984–2012, Horton index (HI) increased as the basin dried up, indicating that vegetation used more of its available water with increasing water limitation in the basin. Q_{50} indicated that discharge is occurring 4.3 days earlier decade^{-1}.

HESSD
12, 7933–7969, 2015

CC BY

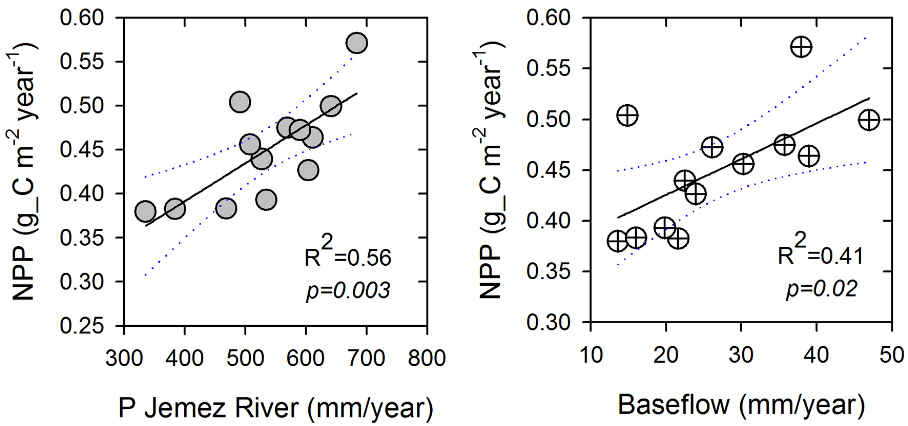

Figure 3. Left panel: positive linear correlation between precipitation in the upper Jemez River Basin and annual NPP in the upper Jemez River Basin derived from MODIS; right panel: linear correlation between baseflow and annual NPP in the upper Jemez River Basin. Forest productivity is water limited in the upper Jemez River Basin. Other variables such as annual, winter and summer air temperature did not correlate with NPP.

HESSD
12, 7933–7969, 2015

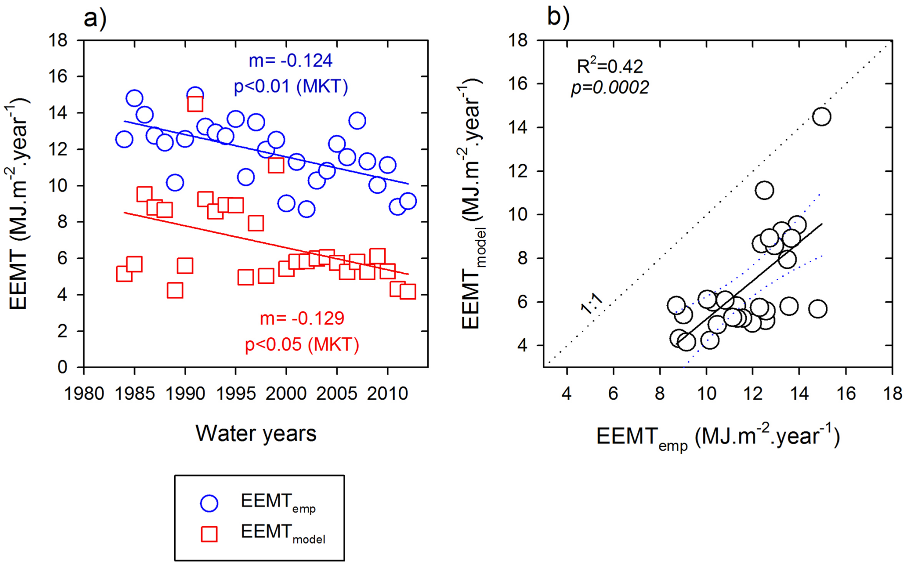

Figure 4. (a) $EEMT_{emp}$ and $EEMT_{model}$ showed similar significant decreasing trends from 1984–2012 of 1.2 and 1.3 $MJ\,m^{-2}\,yr^{-1}$. **(b)** $EEMT_{emp}$ and $EEMT_{model}$ showed a significant linear correlation.

CC BY

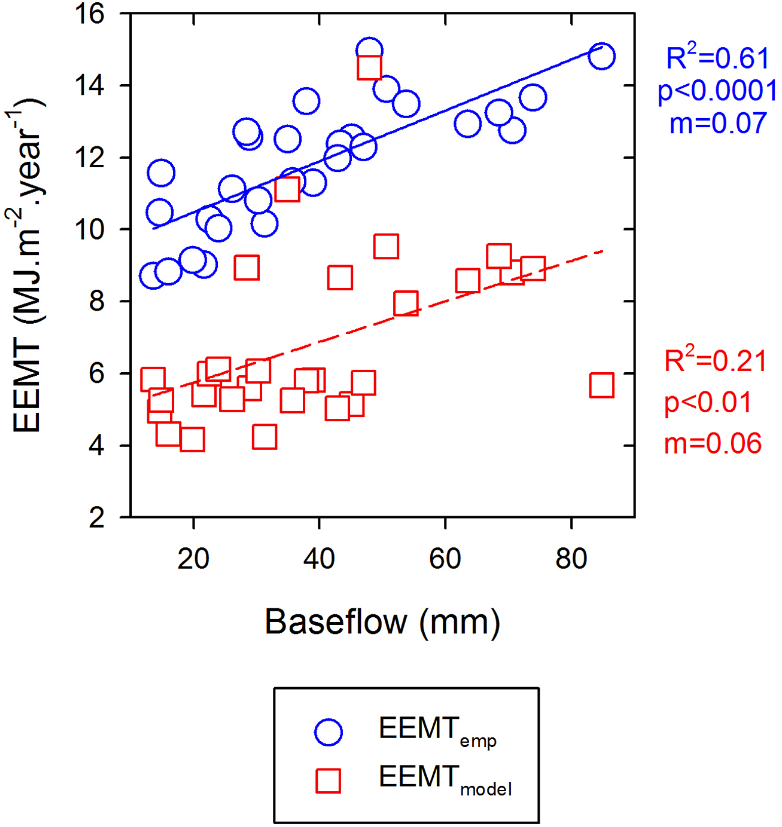

Figure 5. Relationship between water availability and EEMT. Baseflow and EEMT showed a positive linear correlation. As water availability in the Jemez River basin decreases indicated by baseflow, EEMT also decreases.

HESSD
12, 7933–7969, 2015

Influence of climate variability on EEMT in a semi-arid critical zone

X. Zapata-Rios et al.

Title Page
Abstract | Introduction
Conclusions | References
Tables | Figures
Back | Close
Full Screen / Esc
Printer-friendly Version
Interactive Discussion